THE JOURNAL OF BIOLOGICAL CHEMISTRY VOL. 286, NO. 27, pp. 24350–24363, July 8, 2011

Transautocrine Signaling by Membrane Neuregulins Requires Cell Surface Targeting, Which Is Controlled by Multiple Domains*

Received for publication, October 1, 2010, and in revised form, May 5, 2011 Published, JBC Papers in Press, May 13, 2011, DOI 10.1074/jbc.M110.190835

Juan Carlos Montero[1,2,3], **Ruth Rodríguez-Barrueco**[1,3,4], **and Atanasio Pandiella**[5]

From the Instituto de Biología Molecular y Celular del Cáncer-Centro de Investigación del Cáncer, Consejo Superior de Investigaciones Científicas-Universidad de Salamanca, Salamanca 37007, Spain

The neuregulins (NRGs) play important roles in animal development and homeostasis, and their deregulation has been linked to diseases such as cancer and schizophrenia. The NRGs belong to the epidermal growth factor (EGF) family of transmembrane growth factors. Although NRGs may be synthesized as transmembrane proteins (the pro-NRGs), some of them lack an N-terminal signal sequence, raising the question of how these pro-NRGs are directed to the plasma membrane. Here we have explored the domains of pro-NRGs that are required for their membrane anchoring, cell surface exposure, and biological activity. We show that an internal hydrophobic region acts as a membrane-anchoring domain, but other regions of pro-NRG are required for proper sorting to the plasma membrane. Using mutants that are located in different subcellular compartments, we show that only plasma membrane-exposed pro-NRG is biologically active. At this location, the pro-NRGs may act as transautocrine molecules (*i.e.* as membrane factors able to activate receptors present in cells that are in physical contact with the pro-NRG-producing cells (in *trans*) or capable of activating receptors present in the pro-NRG-producing cells (in *cis*)).

The neuregulins (NRGs)[6] are a group of polypeptide growth factors that play critical roles in development (1, 2). Animals lacking NRGs die *in utero* due to heart dysgenesis (3). In addition, a role of NRGs in the control of peripheral nervous system homeostasis has also been demonstrated (4–6). Besides these roles in animal development, deregulation of NRGs has been linked to common diseases, such as cancer (7, 8) and schizophrenia (5). With respect to the former, preclinical studies have shown that expression of NRGs facilitates breast cancer cell proliferation (9), migration, or invasiveness (10, 11), and targeted expression of NRGs in the mammary gland of mice results in the appearance of adenocarcinomas (12). Moreover, increased expression of NRGs has been reported in different types of solid tumors (7), and their presence correlates with the response to some treatments used in the oncology clinic to manage breast cancer (13).

Four NRG genes have been reported (*NRG1* to *-4*), and including all of the different splice variants and NRG isoforms, 30 different NRG isoforms have been described (1, 7). According to the structural components of their N-terminal region, *NRG1* gene isoforms are divided into three different types. NRG1 type I isoforms (also termed heregulin, Neu differentiation factor, or acetylcholine receptor-inducing activity (ARIA)) contain an Ig-like region, followed by a glycosylation-rich segment. The type II isoforms (also known as glial growth factors) lack the glycosylation region while preserving the Ig-like module. Finally, the type III isoforms (sensory and motor-derived factor) lack both domains, which are substituted by a cysteine-rich region. These domains are followed by an EGF-like module, which catalogues the NRGs as part of the EGF family of growth factors (14). This module is exposed to the extracellular milieu in all pro-NRGs except in the case of pro-NRGβ3, which is an intracellular pro-NRG isoform (15). The EGF-like module is followed by a region of substantial variability, termed the linker, that is critical for release of pro-NRGs to the extracellular medium (15–18). The linker of NRGs is followed by a short hydrophobic region, which may act as a membrane anchor and delimitates the extracellular from the intracellular C-terminal domain. According to the length of the C-terminal domain, three subtypes of NRGs have been described: a, b, and c (1).

Most NRGs are biosynthesized as membrane-anchored precursors. These precursor forms are cotranslationally inserted in the membrane of the endoplasmic reticulum and are sorted to the plasma membrane after trafficking through intracellular compartments. Once at the plasma membrane, pro-NRGs may reside at this cellular site, or they may be cleaved to be released as soluble factors by the action of cell surface metalloproteases of the ADAM family (18). Although these biosynthetic and functional properties are shared by other membrane-anchored growth factors, the fact that type I pro-NRGs lack an N-terminal signal sequence (15, 19–22) raises the question of how these pro-NRGs are targeted to the plasma membrane. This question is especially relevant because the N terminus of other EGF fam-

* This work was supported in part by Ministry of Science and Technology of Spain Grants BMC2003-01192, BFU2006-01813/BMC, and BFU2009-07728/BMC. Our Cancer Research Institute receives support from the European Community through the regional development funding program (FEDER/ERDF) and the Fundación Ramón Areces.

[1] Both authors contributed equally to this work.

[2] Supported by the Scientific Foundation of the Spanish Association for Cancer Research.

[3] Supported by the Cancer Center Network Program from the Instituto de Salud Carlos III (RD06/0020/0041).

[4] Recipient of a fellowship from the Spanish Ministry of Education.

[5] To whom correspondence should be addressed: Instituto de Biología Molecular y Celular del Cáncer, Campus Miguel de Unamuno, 37007 Salamanca, Spain. Tel./Fax: 34-923-294815; E-mail: atanasio@usal.es.

[6] The abbreviations used are: NRG, neuregulin; pErbB2 and pErbB3, phosphorylated ErbB2 and ErbB3, respectively; MTT, 3-(4,5-dimethylthiazol-2-yl)-2,5-diphenyltetrazolium bromide; ER, endoplasmic reticulum; PDI, protein-disulfide isomerase; GA, Golgi apparatus.

ily growth factors is expected to direct them to the cell surface. Thus, in the case of proamphiregulin, removal of its N-terminal region, which includes the N-terminal hydrophobic signal sequence, prevents its correct transport to the plasma membrane (23). The intracellular distribution of pro-NRGβ3, an isoform that lacks the internal hydrophobic and C-terminal domains, suggested that these regions could be involved in adequate cell surface sorting of NRGs (15). However, deletion of the linker region of pro-NRGα2c provokes its intracellular retention, indicating that other regions of pro-NRGs may also participate in the sorting of pro-NRGs to the plasma membrane (17).

Cell surface membrane-bound pro-NRGs retain biological activity, indicating that cleavage of the transmembrane protein may not be critical for its activity (9, 17, 24). This conclusion is based on experimental systems in which uncleavable pro-NRGs have been demonstrated to activate the NRG receptors (the ErbB/HER family of receptors) on adjacent cells (in *trans* or juxtacrine) (17, 24). However, whether pro-NRGs may activate ErbB receptors present in the same cell that produces the transmembrane NRG (in *cis* or autocrine) is not known. Some precedents of this kind of interaction have been reported in the case of the related family member pro-EGF. Thus, intracellular entrapment of pro-EGF has been reported to activate the EGF receptor (25, 26). This property, termed intracrine stimulation, may promote migration of mammary epithelial cells (27). It is therefore possible that pro-NRGs, which are expected to travel to the cell surface crossing the same intracellular compartments as the cognate receptors, may behave analogously.

In this paper, we have performed molecular as well as biological analyses to define the domains of pro-NRGs required for their adequate cell surface exposure and biological actions. In addition, we investigated whether membrane-anchored pro-NRGs are functional while traveling along their biosynthetic route. Finally, we also explored whether pro-NRGs can activate their receptors in *cis*.

EXPERIMENTAL PROCEDURES

Reagents and Immunochemicals—Culture media, sera, and G418 were purchased from Invitrogen (Carlsbad, CA). Protein A-Sepharose was from Amersham Biosciences. Immobilon-P membranes were from Millipore Corp. (Bedford, MA). DAPI, brefeldin A, proteinase K, protein A-HRP, and doxycycline were from Sigma. TAPI-2 was from Calbiochem. Wheat germ agglutinin-agarose was from GE Healthcare. Other generic chemicals were purchased from Sigma, Roche Applied Science, or Merck.

The anti-NRG endodomain antibody was raised against the sequence NH_2-CETPDSYRSDPHSER-COOH, which corresponds to the C-terminal residues of rat NRGα2c (18). For the generation of the anti-NRG ectodomain antibody, rabbits were immunized with a GST fusion protein that included amino acids 19–181 of rat NRGα2c (17). The anti-phospho-Akt antibody was raised in our laboratory and recognizes the sequence NH_2-CRPHFPQFpSYSAS-COOH. Anti-Akt, anti-phospho-Erk1/2, anti-Erk2, anti-GAPDH, anti-ErbB3, anti-ErbB4, and anti-phosphotyrosine antibodies were from Santa Cruz Biotechnology, Inc. (Santa Cruz, CA). The anti-Erk5 antibody was generated in our laboratory (28). The Ab3 antibody used to detect ErbB2 in Western blots was from Calbiochem-Merck. The monoclonal antibody anti-ErbB2 ectodomain as well as recombinant NRG were generously provided by Dr. Mark X. Sliwkowsky (Genentech, San Francisco, CA). The anti-pErbB2 antibody was from Cell Signaling (Cambridge, MA). The anti-HA antibody was from Roche Applied Science. Trastuzumab was obtained from a local pharmacy. Antibodies against calnexin and protein-disulfide isomerase (PDI) were obtained from Stressgen (San Diego, CA). Antibodies to GM130 and p230 were from BD Transduction Laboratories (Lexington, KY). The Cy3- or Cy2-conjugated antibodies were purchased from Jackson Immunoresearch (West Grove, PA), and Alexa 488-conjugated antibodies were from Invitrogen. HRP conjugates of anti-rabbit or anti-mouse IgG were from Bio-Rad. The Alexa 546 kit used for the labeling of anti-ErbB3 and -pErbB2 antibodies was from Invitrogen. The anti-pErbB2 antibody was raised against the sequence NH_2-CSPQPEpYVNQPD-COOH of human ErbB2 phosphorylated at tyrosine 1139. For the generation of the anti-ErbB3 antibody, rabbits were immunized with a GST fusion protein that included 166 intracellular amino acids of human ErbB3.

Cell Culture and Transfections—The conditions for the culture of MCF7 and 293 cells have been described previously (17). Transfections in 293 or MCF7 cells were performed by calcium phosphate (29) or using Lipofectamine (Invitrogen), respectively. Clones were selected by G418 resistance, and their NRG expression was analyzed by Western blotting. The MCF7-NRGα2c^{tetoff} clone has been described previously (9).

Plasmids—The plasmid containing the whole sequence of rat pro-NRGα2c (pcDNA3-NRGα2c) was generated by double digestion with KpnI and NotI restriction enzymes. NRGα2c$^{\Delta Ig}$ mutant was generated by digesting the pcDNA3-NRGα2c construct with BamHI because the immunoglobulin domain is surrounded by sites for this enzyme. Other mutants were generated by PCR using the following primers: NRG$^{\Delta intra}$ (forward, 5′-AAG CTT ATG TCT GAG CGC AAA GAA GG-3′; reverse, 5′-G CCG ATC AAG CTT TTA CCG CTG CTT CTT GG-3′), NRG$^{\Delta extra}$ (forward, 5′-AG GAA TCC GTG CTG ACA ATT ACT G-3′; reverse, 5′-TAT TCT AGA TTA CCT TTC GCT ATG AGG-3′), NRGβ3-like (forward, 5′-AAG CTT ATG TCT GAG CGC AAA GAA GG-3′; reverse, 5′-CC AAG CTT TTA GTA GAG TTC CTC CGC TTT TTC-3′). PCR products were digested with HindIII, EcoRI, or XbaI and subcloned in the pcDNA3 vector (Invitrogen). To obtain clones of the mutants that can be reprimed, sequences were subcloned in the pRevTRE vector (BD Biosciences) after PCR amplification and SalI combined with ClaI (NRGβ3-like) or HindIII (NRG$^{\Delta intra}$) digestion. The NRGα2c-GFP fusion protein was generated by PCR using the following primers: forward, 5′-ACC CTC GAG ATG TCT GAG CGC AAA GAA GGC-3′; reverse, 5′-TTT GAA TTC GCC CTT TCG CTA TGA GGA GA-3′. The PCR product was digested with XhoI and EcoRI and subcloned in the plasmid pEGFP-N3 (BD Biosciences).

Chimeras of HA-ERK5 with different regions of pro-NRGα2c were constructed as follows. The HA-ERK5 full-length cDNA was amplified using the primers 5′-AAG CTT ATG TAC GAC GTT CCT GAT-3′ (forward) and 5′-CTC

GAG GGG GTC CTG GAG GTC-3′ (reverse), digested with HindIII and XhoI, and subcloned into pCDNA3. For the construction of HA-ERK5-NRGα2c, the stop codon of ERK5 was eliminated to allow in frame continuation of protein synthesis of the transmembrane and intracellular regions of pro-NRGα2c. These regions of pro-NRGα2c, corresponding to amino acids 231–422, were PCR-amplified with the primers 5′-CTC GAG ACC CAA GAA AAA GCG-3′ (forward) and 5′-TCT AGA TTA CCT TTC GCT ATG AGG-3′ (reverse) and fused to the C terminus of HA-ERK5. To create the chimera containing the ectodomain plus transmembrane region of pro-NRGα2c, the region coding for amino acids 1–273 was PCR-amplified using the primers 5′-AAG CTT ATG TCT GAG CGC AAA GAA GG-3′ (forward) and 5′-TCT AGA TTA CCT TTC GCT ATG AGG-3′ (reverse) and fused to the N terminus of HA-ERK5 (forward, 5′-AAG CTT ATG TAC GAC GTT CCT GAT-3′; reverse, 5′-TCT AGA TCA GGG GTC CTG GAG GTC-3′). Construction of the HA-ERK5-TMα2c was prepared by PCR-amplifying amino acids 231–267 of pro-NRGα2c using the primers 5′-CTC GAG ACC CAA GAA AAA GCG-3′ (forward) and 5′-TCT AGA TTA CTG CCG CTG CTT CTT GGT-3′ (reverse), and the resulting fragment was fused to the C terminus of HA-ERK5 (forward, 5′-AAG CTT ATG TAC GAC GTT CCT GAT-3′; reverse, 5′-CTC GAG GGG GTC CTG GAG GTC-3′).

Metabolic Labeling—MCF7-NRGα2c or MCF7-NRG$^{\Delta intra}$ cells were plated in 100-mm dishes and grown to 80% confluence. Cells were washed twice for 20 min each with methionine- and cysteine-free DMEM and then were incubated in the same medium containing 200 μCi/ml of a mixture of [^{35}S]methionine and [^{35}S]cysteine (EasyTag^{TM} Express35S protein labeling mix, PerkinElmer Life Sciences) for 20 min. The radioactive medium was replaced with fresh complete medium, and cells were chased for the indicated times. Cells were lysed, and then lysates were precleared by the addition of 50 μl of protein A-Sepharose. After incubation at 4 °C for 30 min in a rocking platform, the lysates were centrifuged at 10,000 × *g* for 10 s, and the supernatants were transferred to new tubes containing the antibodies (anti-endodomain antibody to precipitate pro-NRGα2c or anti-NRG to precipitate NRG$^{\Delta intra}$). Lysates were incubated for 2 h at 4 °C, and then 50 μl of protein A-Sepharose were added for an additional 30 min. The precipitates were washed five times with radioimmune precipitation buffer and boiled in electrophoresis sample buffer. Samples were run in 8% (for pro-NRGα2c) or 10% (for NRG$^{\Delta intra}$) SDS-polyacrylamide gels that were fixed and dried before exposure to autoradiographic film or PhosphorImager screens for quantitative analyses.

Immunoprecipitation and Western Blotting—Cells were washed with PBS and lysed in ice-cold lysis buffer (140 mM NaCl, 10 mM EDTA, 10% glycerol, 1% Nonidet P-40, 20 mM Tris (pH 7.0), 1 μM pepstatin; 1 μg/ml aprotinin, 1 μg/ml leupeptin, 1 mM PMSF, and 1 mM sodium orthovanadate). After scraping the cells from the dishes, samples were centrifuged at 10,000 × *g* at 4 °C for 10 min, and supernatants were transferred to new tubes. Immunoprecipitations were performed with the corresponding antibody and protein A-Sepharose at 4 °C for at least 2 h, and the immune complexes were recovered by a short centrifugation followed by three washes with 1 ml of cold lysis buffer. Samples were then boiled in electrophoresis sample buffer and loaded in SDS-polyacrylamide gels. After transfer to PVDF membranes, these were blocked for 1 h in Tris-buffered saline with tween containing 1% BSA and then incubated for 2–16 h with the corresponding antibody. After washing with Tris-buffered saline with tween, membranes were incubated with HRP-conjugated secondary antibodies for 30 min and washed, and bands were visualized by a luminol-based system with *p*-iodophenol enhancement (30).

Subcellular Fractionation—Cell fractionation experiments were performed as described previously (31). Cells grown in 100-mm dishes until 90% of confluence were washed twice with PBS and incubated for 10 min with 0.25 M sucrose, 1 mM EDTA, 1 mM PMSF, and 10 mM Tris, (pH 7.0). The cell suspension was homogenized on ice with a tightly fitting Dounce homogenizer (50 strokes) and centrifuged at 4,000 × *g* for 10 min. The resulting pellet was rehomogenized and centrifuged at the same speed. The supernatants from these centrifugation steps were pooled and centrifuged at 30,000 × *g* for 30 min. The supernatant was considered the cytosolic fraction, and the pellet was considered the microsomal fraction.

Immunofluorescence and FRET Experiments—Cells cultured on glass coverslips were washed with PBS and fixed in 2% *p*-formaldehyde for 30 min at room temperature, followed by two rinses in PBS. Monolayers were then permeabilized three times for 10 min each with PBS supplemented with 0.1% (final concentration) Triton X-100 and then blocked twice in PBS with 0.2% BSA for 10 min each at room temperature. Cells were incubated with the indicated primary antibodies in blocking solution for 2 h at room temperature or overnight at 4 °C. After three washes for 10 min each in PBS with 0.2% BSA, coverslips were incubated with Cy3- or Alexa 488-conjugated secondary antibodies for 30 min and washed three times in PBS with 0.2% BSA. Immunolabeled cells were counterstained with DAPI to detect cell nuclei, and then the slides were mounted. Samples were analyzed by regular epifluorescence microscopy or by confocal immunofluorescence microscopy using a Zeiss LSM510 system. To avoid interference between fluorescence signals, confocal images were captured under multitracking mode.

MCF7 cells expressing NRG-GFP were cultured on glass coverslips. EGFP fluorescence was excited with the argon 476-nm laser line and detected between 487 and 540 nm, whereas Alexa 546 was excited at 561 nm and detected between 571 and 680 nm. To minimize cross-talk between the channels, each image was collected separately in the multitrack mode. Acceptor photobleaching was achieved by scanning 20 times a region of interest using the 561-nm laser line at 100% intensity. To minimize the effect of photobleaching of the donor during the imaging process, the image acquisition was performed at low intensities. FRET efficiency was measured after photobleaching of the Alexa 546 fluorochrome bound to anti-pErbB2 or anti-ErbB3 antibody, using the software Leica LAS AF (Leica). The results are plotted as the mean ± S.D. of arbitrary units obtained in three different experiments in which at least 10 distinct areas per experiment and condition were analyzed.

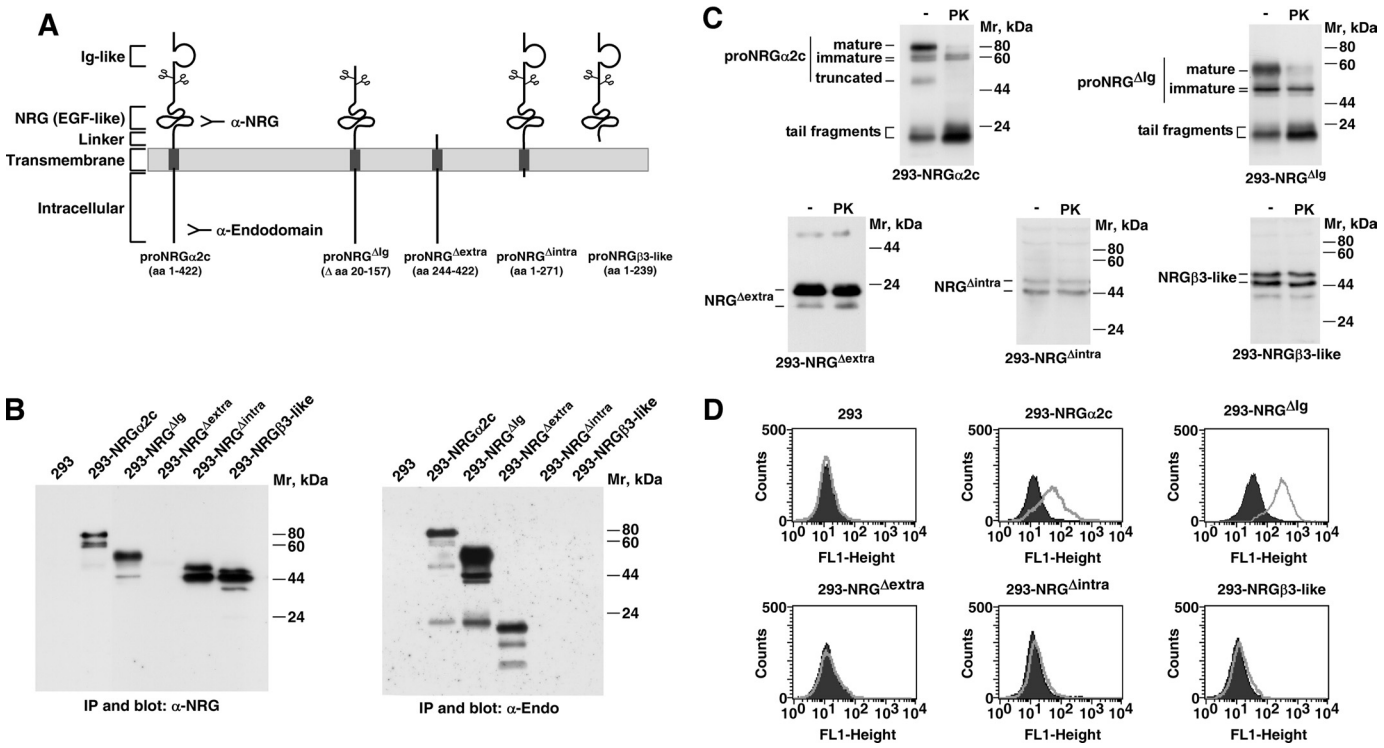

FIGURE 1. **Expression and analyses of cell surface exposure of different pro-NRGα2c forms.** *A*, schematic representation the different mutants of pro-NRGα2c, also indicating the number of amino acids of each construction and regions recognized by the two different anti-NRG antibodies used. *B*, expression of the different mutants in 293 cells. 293 cells transfected with the cDNA coding for the different mutants were lysed, and cell extracts were immunoprecipitated (*IP*) with the anti-NRG or anti-endodomain antibodies. The samples were run on SDS-polyacrylamide gels that were transferred to PVDF membranes. The blots were probed with the same antibodies used to immunoprecipitate the samples. The position of the M_r markers is shown at the *right*. *C*, protease protection experiments. Intact 293 cells expressing the different mutants were treated with or without proteinase K (*PK*; 200 μg/ml) for 30 min and lysed. The samples were analyzed by Western blot with the anti-endodomain or anti-NRG antibodies. *D*, FACS analyses of NRG cell surface exposure. Cells were incubated with the anti-NRG antibody followed by an anti-rabbit antibody conjugated to FITC. Fluorescence intensity was measured with a FACSCalibur Flow cytometer. *Filled histograms* correspond to signals from cells incubated with the secondary antibody alone, whereas *gray line histograms* represent the fluorescence due to the expression of different NRG forms. *aa*, amino acids.

Analysis of Cell Surface Pro-NRG—Cell surface expression of NRG mutants was determined by FACS using the anti-NRG ectodomain antibody. Cells were washed twice with PBS, scraped, and collected into 15-ml tubes. Then they were washed again with PBS and resuspended in 1 ml of PBS containing 2% BSA and 2 μl of the anti-NRG antibody. After 1 h of incubation at room temperature, cells were washed twice and resuspended in PBS/BSA containing the secondary anti-rabbit IgG antibody conjugated to FITC. After a 30-min incubation, the cells were washed with PBS. Finally, the mean light intensity was measured using the CellQuest application in a FACSCalibur cytometer (BD Biosciences).

MTT Metabolization Assays—Subconfluent monolayer cultures were trypsinized, and cells were plated in 24-well plates to a density of 20,000 cells/well and cultured overnight in DMEM plus 10% FBS. The next day, the medium was replaced with DMEM without FBS, with or without the indicated treatment. Cell proliferation was analyzed at 3 days by an MTT-based assay as described (9). The results are presented as the mean ± S.D. of quadruplicates of a representative experiment that was repeated at least three times.

Statistics and Quantitative Estimation of Pro-NRG Forms—Results obtained in the proliferation experiments are represented as the mean ± S.D. of at least three independent experiments. Significance was considered when p values were <0.05.

Quantitation of the different pro-NRG forms in gels from radioactive pulse-chase experiments was performed using the Quantity One software version 4.1.1 (Bio-Rad). Quantitation of the autoradiographic bands obtained from Western blot experiments was performed using the ImageJ version 1.44 software (National Institutes of Health, Bethesda, MD). The intensity of each of the different bands was calculated, and the sum of all in each lane was obtained. Data are represented as the percentage of the maximum value obtained for each experiment.

RESULTS

Plasma Membrane Sorting of Pro-NRGα2c Mutants—Using pro-NRGα2c as a model for the study of type I transmembrane NRGs, we formerly reported that a small region in the extracellular juxtamembrane domain controlled its sorting to the plasma membrane (17). To identify additional domains that may also participate in membrane sorting and/or membrane anchoring of pro-NRGα2c, we used a strategy based on the creation of various deletion mutants that eliminated different regions of the intracellular or extracellular domains (Fig. 1*A*). Mutants of the ectodomain included the pro-NRG$^{\Delta Ig}$, in which the Ig-like domain has been deleted, and the pro-NRG$^{\Delta extra}$ form, in which the extracellular domain has been removed. The pro-NRG$^{\Delta intra}$ form was created by removing the intracellular domain of pro-NRGα2c. The pro-NRGβ3-like form was cre-

ated by a stop codon that interrupted reading of pro-NRGα2c right before the internal hydrophobic region, to mimic pro-NRGβ3 (1). cDNAs coding for these different deletion mutants were transfected into 293 cells, and expression was assessed with antibodies that detect either the ectodomain or the intracellular C terminus of pro-NRGα2c. As shown in Fig. 1*B*, Western blotting with the anti-ectodomain antibody recognized all of the mutants, except the pro-NRG$^{\Delta extra}$ form. As expected, the latter was, however, recognized by the anti-endodomain antibody, which also recognized wild type pro-NRGα2c or the pro-NRG$^{\Delta Ig}$ mutant. Pro-NRGβ3-like as well as the pro-NRG$^{\Delta intra}$ forms were only recognized by the anti-ectodomain antibody. Both the anti-ectodomain and anti-endodomain antibodies recognized several bands that correspond to distinct molecular forms. In fact, in the case of the wild type pro-NRGα2c form, former studies indicated that its expression in 293 cells resulted in the presence of a slower migrating band that corresponds to mature pro-NRGα2c (Fig. 1*C*) (17, 18) together with two other immature, intracellular bands that migrate faster. In addition, we frequently detect another pro-NRGα2c form that corresponds to a truncated version. Finally, a group of smaller M_r bands solely detected by the anti-endodomain antibody are also present and are generated by cleavage of the ectodomain of pro-NRGα2c. These forms correspond to cell-associated tail fragments devoid of the NRG-EGF-like domain (18).

Proteinase K treatment of intact pro-NRGα2c-expressing cells has been used to determine plasma membrane exposure of this progrowth factor (17, 18). In fact, treatment with proteinase K strongly decreased the amounts of the mature and the truncated forms, indicating that they were exposed at the cell surface (Fig. 1*C*). In contrast, the amount of the lower M_r immature forms remained unchanged upon treatment with the protease, confirming that these forms are intracellular and are therefore protected from the action of the protease. Treatment of cells expressing the pro-NRG$^{\Delta Ig}$ mutant yielded analogous results; the slowest migrating band was sensitive to treatment with proteinase K, whereas the slightly faster migrating forms were insensitive. In 293 cells expressing either the wild type pro-NRGα2c or the pro-NRG$^{\Delta Ig}$ mutant, treatment with protease K resulted in an increase in the amount of the cell-associated tail fragments. Protease K treatment of 293 cells expressing the pro-NRG$^{\Delta intra}$, the pro-NRG$^{\Delta extra}$, or the pro-NRGβ3-like forms did not cause a detectable effect on the amount of any of the forms expressed.

We further inspected plasma membrane exposure of the distinct mutants by flow cytometry using the anti-ectodomain antibody. As shown in Fig. 1*D*, staining indicative of cell surface exposure was observed for wild type pro-NRGα2c or the pro-NRG$^{\Delta Ig}$ mutant but not in the case of pro-NRG$^{\Delta intra}$ or the pro-NRGβ3-like forms. The pro-NRG$^{\Delta extra}$ form, because it lacks the extracellular domain, could not be detected by the antiectodomain antibody, and therefore this technique could not be used to define whether this form reached the plasma membrane. Taken together, these data indicated that pro-NRGα2c or pro-NRG$^{\Delta Ig}$ was targeted to the plasma membrane, but pro-NRG$^{\Delta intra}$ and the pro-NRGβ3-like forms failed to reach this location.

Membrane-anchoring Properties of Pro-NRGα2c Mutants—To analyze the membrane-anchoring properties of the different pro-NRGα2c mutants, we performed a simple subcellular fractionation procedure to segregate the light (cytosolic fraction) from the heavy (microsomal) fractions. The nuclear compartment was not isolated for analysis in these experiments. Wild type pro-NRGα2c, pro-NRG$^{\Delta Ig}$, pro-NRG$^{\Delta extra}$, and pro-NRG$^{\Delta intra}$ associated with the heavy fraction (Fig. 2*A*). The pro-NRGβ3-like form was present in the cytosolic fraction but not in microsomes, indicating that this form, in contrast to the other mutants tested, was unable to tightly associate to cellular membranes. Western blotting of samples from each fraction with markers of cytosol (GAPDH) or microsomes (calnexin) confirmed the separation between both fractions.

The above data indicated that the internal hydrophobic region of pro-NRGα2c was required and sufficient for membrane anchoring. We next asked whether that region had sufficient strength to target a protein to the plasma membrane or could confer membrane-anchoring properties to a cytosolic protein. To address this, we created several chimeras of pro-NRGα2c and ERK5 (schematically represented in Fig. 2*B*). ERK5 is a member of the MAPK family of signal transducers and mainly locates in the cytosolic compartment (32). One of the chimeras included the ectodomain and the transmembrane region of pro-NRGα2c (residues 1–273) fused to HA-ERK5 (NRGα2c-ERK5). A second chimera, which was named ERK5-NRGα2c, included HA-ERK5 fused to the transmembrane and intracellular regions of pro-NRGα2c (residues 231–422). Finally, a third chimera (ERK5-TMα2c) consisted of ERK5 fused to the minimal internal hydrophobic region of pro-NRGα2c (residues 231–267). 293 cells were transfected with the cDNAs coding for these different mutants, and their expression was analyzed by Western blotting using anti-HA to differentiate endogenous from exogenous ERK5 or using anti-ERK5 to detect endogenous ERK5 that we used as a control for the cytosolic fraction. The distinct M_r between endogenous ERK5 and the chimeras allowed us to use it for that purpose. Cell fractionation experiments indicated that ERK5-NRGα2c, NRGα2c-ERK5, and ERK5-TMα2c associated with the microsomal fraction, whereas endogenous ERK5 was mainly cytosolic (Fig. 2*C*). We also explored whether the chimeras reached the plasma membrane. Proteinase K protection experiments indicated that none of these three chimeras was able to be exposed at the plasma membrane because they offered resistance to treatment with the protease (Fig. 2*D*). Moreover, immunofluorescence experiments with an anti-HA antibody showed intracellular staining of all of these chimeric proteins (Fig. 2*E*). Together, these data supported the concept that the internal hydrophobic region of pro-NRGα2c is strong enough to drive membrane association of a protein but is unable to force the expression of any protein at the plasma membrane.

Subcellular Location of the Pro-NRGα2c Mutants—We proceeded to explore the subcellular location of the different mutants by immunofluorescence microscopy. These analyses confirmed previously published data on the subcellular distribution of pro-NRGα2c, which was located at the plasma membrane and the Golgi apparatus because it colocalized with the Golgi marker GM130 (17) (Fig. 3*A*). The distribution obtained

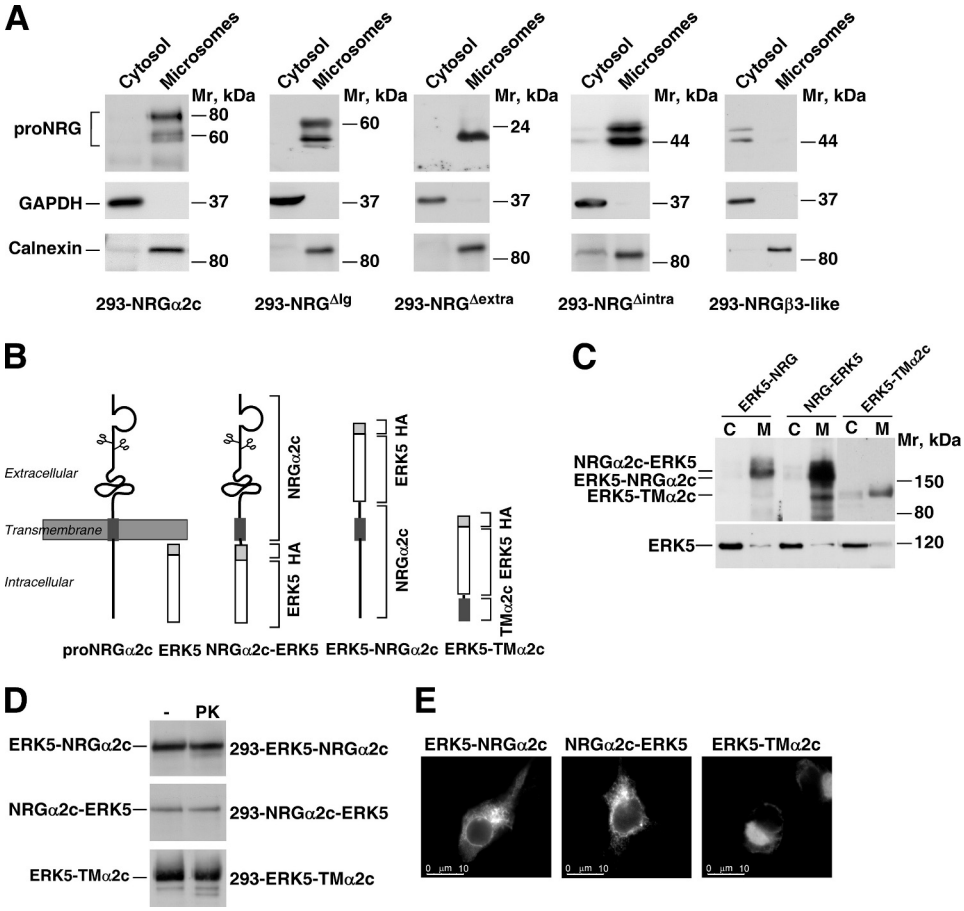

FIGURE 2. **The internal hydrophobic region of pro-NRGα2c is responsible for its membrane anchoring.** *A*, cell fractionation experiments of the different mutants of pro-NRGα2c. Cells expressing the different forms were fractionated as described under "Experimental Procedures," and cytosolic or microsomal fractions were analyzed for pro-NRG, GAPDH, and calnexin by Western blot. The position of the *M*, markers is shown at the *right*. *B*, schematic representation of ERK5-NRGα2c, NRGα2c-ERK5, and ERK5-TMα2c chimeras. *C*, the cytosolic (*C*) and microsomal (*M*) compartments of 293 cells transfected with the cDNA coding for the different chimeras were analyzed for pro-NRGα2c and ERK5 by Western blot. *D*, 293 cells expressing the different chimeras were treated with proteinase K (*PK*). The cell extracts were immunoprecipitated with the anti-HA antibody, and the Western blots were analyzed with the same antibody. *E*, immunofluorescence analysis of the subcellular distribution of the chimeric proteins in 293 cells, in which these proteins were stained with the anti-HA antibody.

with the pro-NRG$^{\Delta Ig}$ mutant was very similar to that of the wild type protein. Staining of 293 cells expressing the pro-NRG$^{\Delta extra}$ form revealed a pattern consistent with this mutant being located at the plasma membrane (Fig. 3*A*). Previously, it has been proposed that pro-NRGβ3 was a nuclear protein (15). In line with this, the immunofluorescence data indicated that this form was located in a region that corresponded to the nuclear compartment because it colocalized with DAPI staining (Fig. 3*B*).

Pro-NRG$^{\Delta intra}$ colocalized with Golgi markers (GM130 and p230), and also some colocalization was observed with the ER marker PDI (Fig. 3*C*). No clear plasma membrane location was observed. Although the pro-NRG$^{\Delta intra}$ was associated with the microsomal fraction, its failure to move to the plasma membrane could be affected by defective entry into the lumen of the ER (*e.g.* by failure to translocate the N terminus to the lumen, therefore leaving that region exposed to the cytosolic compartment). To investigate this, we took into consideration the fact that entry of pro-NRGα2c into the ER luminal compartment is accompanied by glycosylation (17). To follow this posttranslational modification, we performed wheat germ agglutinin precipitation of the pro-NRG$^{\Delta intra}$ form and compared it with wild type pro-NRGα2c, pro-NRG$^{\Delta extra}$, and the pro-NRGβ3-like form. The latter two forms were used as controls because one of them (pro-NRG$^{\Delta extra}$) lacks the ectodomain, and the other is not membrane-associated (pro-NRGβ3-like). Wheat germ agglutinin efficiently precipitated wild type pro-NRGα2c as well as pro-NRG$^{\Delta intra}$ mutant (Fig. 3*D*). In contrast, wheat germ agglutinin failed to precipitate the pro-NRGβ3-like and pro-NRG$^{\Delta extra}$ forms.

Biological Properties of the Different Pro-NRGα2c Mutants—Because previous reports on mutant pro-EGF forms indicated that intracellularly trapped pro-EGF was biologically active (25, 27), we decided to explore whether intracellular pro-NRG behaved analogously. In addition, we also attempted to elucidate whether pro-NRGβ3 was active in terms of proliferation. Previously, we established a system for the evaluation of the biological properties of membrane-anchored pro-NRGs, using MCF7 cells as a reporter cell line (9). This cell line expresses levels of ErbB/HER receptors that are analogous to those present in the normal breast epithelium (33) and responds mitogenically to soluble NRG (34). Furthermore, expression of wild type pro-NRGα2c in these cells strongly stimulates their proliferation (9). We therefore created

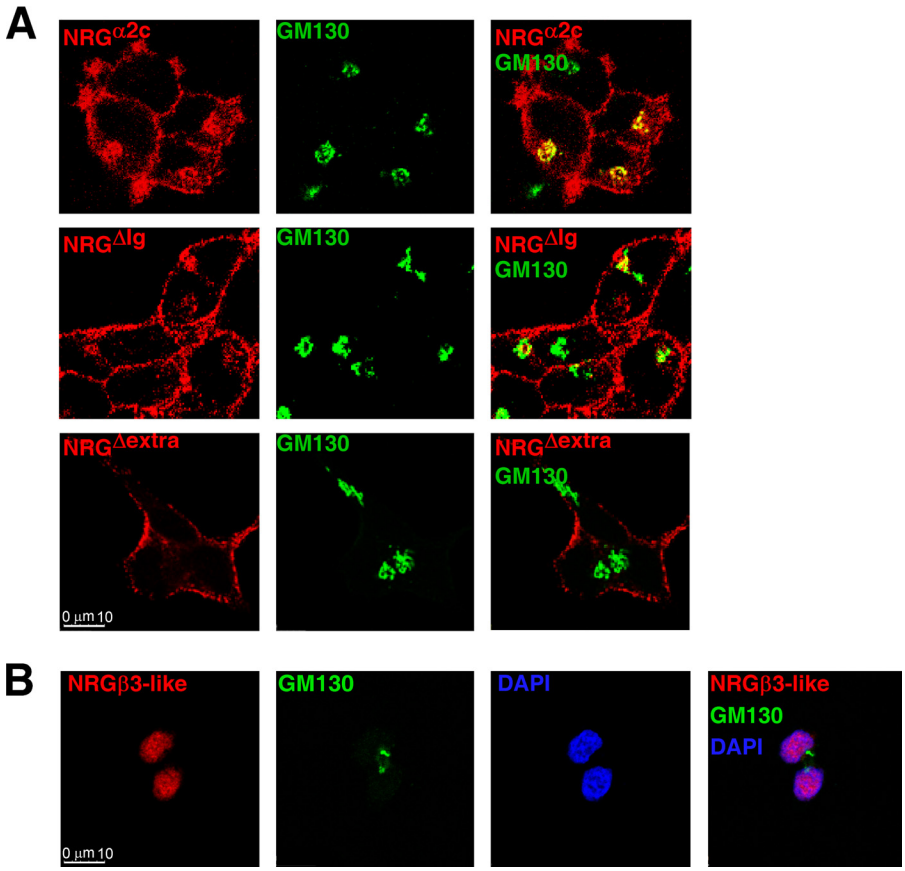

FIGURE 3. **Subcellular localization of pro-NRGα2c mutants.** Distribution of pro-NRGα2c, pro-NRG$^{\Delta Ig}$, and pro-NRG$^{\Delta extra}$ (*A*) and NRGβ3-like (*B*) in 293 cells was assessed by immunofluorescence using the anti-NRG or anti-endodomain antibodies as described under "Experimental Procedures." Golgi apparatus localization was determined by immunofluorescence using an anti-GM130 antibody, and nuclear staining was performed with DAPI. *C*, detection of the pro-NRG$^{\Delta intra}$ mutant in 293 cells by immunofluorescence with the anti-endodomain antibody. Colocalization with the *cis*-Golgi was determined using anti-GM130 antibody, and colocalization with the *trans*-Golgi apparatus was determined with the anti-P230 antibody. The endoplasmic reticulum was stained with the anti-protein-disulfide isomerase (*PDI*) antibody. *D*, glycosylation of different pro-NRGα2c mutants. Protein extracts of 293 cells expressing each construct were precipitated with wheat germ agglutinin-agarose (*WGA*) for 2 h and centrifuged, and complexes were resolved in a 10% SDS-polyacrylamide gels. Detection of pro-NRG forms was carried out by Western blot using the anti-ectodomain and anti-endodomain antibodies.

MCF7 derivatives from the parental cell line MCF7^{tetoff}, in which expression of the different pro-NRG forms to be analyzed (pro-NRGα2c, pro-NRG$^{\Delta intra}$, and pro-NRGβ3-like) could be regulated by the addition of the tetracycline analog doxycycline. This strategy was chosen to avoid clonal differences between the distinct transfectants. We did not contemplate further analysis of pro-NRG$^{\Delta Ig}$ mutant because in previous cell biological experiments it behaved as the pro-NRGα2c wild type protein. Expression of the different forms in distinct clones and their repression by doxycycline were assessed by Western blotting with the anti-ectodomain antibody, and clones with analogous levels were selected for further studies (Fig. 4*A*). Two different clones of each cell line were used, although the data described below correspond to a representative one.

Immunofluorescence studies revealed that the subcellular location of these mutants in MCF7 cells offered a distribution analogous to that observed in 293 cells (Fig. 4*B*). To analyze the proliferation properties of MCF7 cells expressing the different pro-NRG forms, we performed MTT metabolization studies. In these experiments, we used exogenous NRG as a control for the maximum growth factor-induced proliferation. MCF7^{tetoff} cells, which represented the parental cell line from which clones of the different pro-NRG forms were obtained, had low proliferation in serum-free conditions, and this proliferation was unaffected by the addition of doxycycline (Fig. 4*C*). The addition of NRG resulted in a strong proliferation response that was also unaffected by the addition of doxycycline. MCF7-NRGα2c cells efficiently proliferated in serum-depleted culture medium, and the proliferation was strongly inhibited by the addition of doxycycline. The amount of proliferation obtained with the expression of wild type pro-NRGα2c was analogous to that obtained by supplementing the culture medium with exogenous soluble NRG. The action of the latter was similar in cells treated with doxycycline, indicating that this compound did not affect the response of the cells to NRG and suggesting that the decrease in proliferation in the presence of doxycycline is in fact due to repression of pro-NRGα2c synthesis. In contrast to MCF7-NRGα2c cells, MCF7 cells expressing pro-NRG$^{\Delta intra}$ or pro-NRGβ3-like forms had very low proliferation, analogous to that of wild type untransfected MCF7 cells. Moreover, MCF7-NRG$^{\Delta intra}$ and MCF7-NRGβ3-like cells failed to proliferate when expression of the two mutant forms was allowed. However, stimulation of these cell lines with exogenous NRG increased their MTT metabolization to levels analogous to those observed in untreated or NRG-treated MCF7-NRGα2c

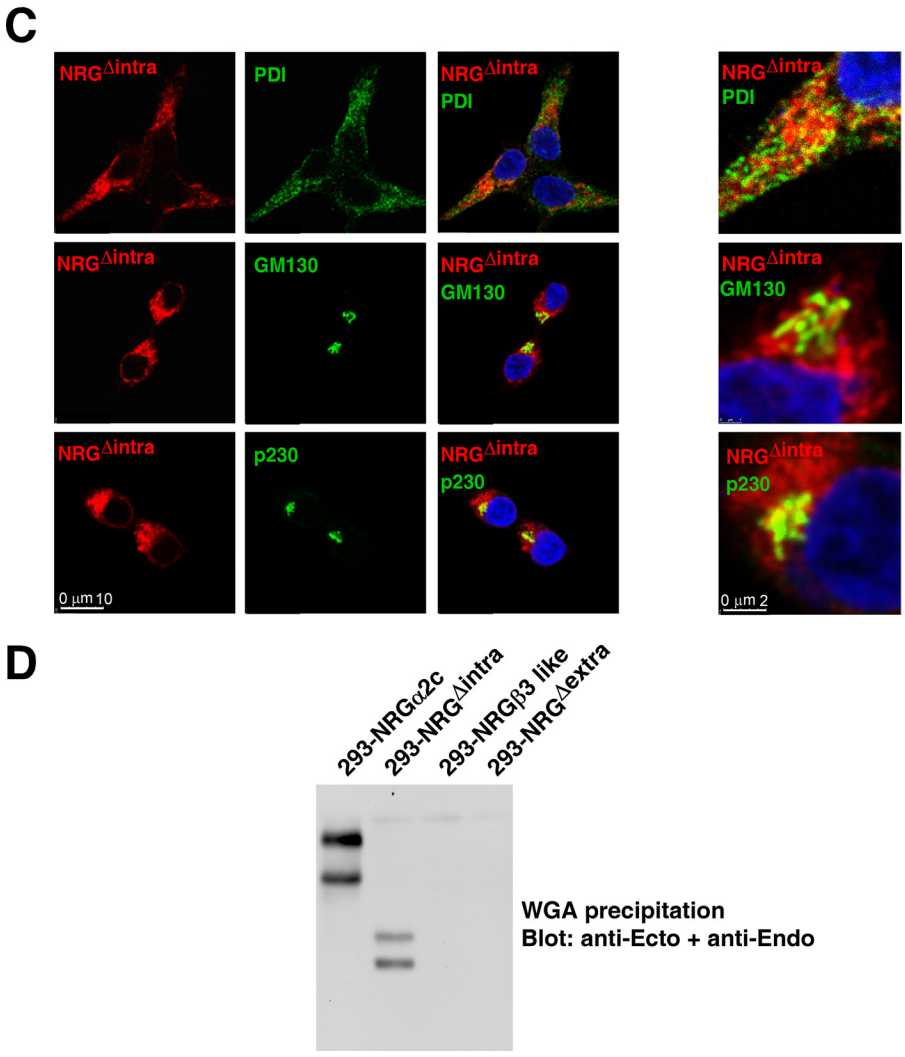

FIGURE 3—*continued*

cells, indicating that MCF7^{tetoff} cells expressing those two mutant forms retained the capability to mitogenically respond to exogenously added NRG.

We also explored the proliferation of MCF7-NRG$^{\Delta intra}$ and MCF7-NRGβ3-like cells in response to trastuzumab, a monoclonal antibody designed to the extracellular domain of HER2. This antibody has formerly been shown to prevent proliferation of MCF7-NRGα2c cells because it uncouples pro-NRGα2c-ErbB receptor interaction (9). Treatment with this antibody efficiently prevented proliferation of MCF7-NRGα2c cells but did not affect proliferation of MCF7-NRG$^{\Delta intra}$ and MCF7-NRGβ3-like cells (Fig. 5*A*). Remarkably, the MTT metabolization values reflecting inhibition of proliferation of MCF7-NRGα2c cells treated with trastuzumab reached values analogous to those obtained in MCF7-NRG$^{\Delta intra}$ and MCF7-NRGβ3-like cells.

To analyze whether these biological differences in terms of cell proliferation also reflected differences in signaling, we explored the activation state of HER receptors and intracellular signaling pathways related to cell proliferation/survival in MCF7 cells. ErbB2, ErbB3, and ErbB4 were constitutively phosphorylated in tyrosine residues in MCF7-NRGα2c cells but not in the other cell lines (Fig. 5*B*). This level of phosphorylated ErbB receptors was regulated by doxycycline, indicating that such activation of ErbB receptor tyrosine phosphorylation depended upon the expression of pro-NRGα2c. In contrast, the resting phosphorylation in tyrosine residues of these receptors was very low in MCF7-NRG$^{\Delta intra}$ and MCF7-NRGβ3-like cells and was insensitive to doxycycline. Analogously, resting phospho-Akt phosphorylation at Ser^{473} and dual phosphorylation of Erk1/2 were also detected in MCF7-NRGα2c cells but not in MCF7-NRG$^{\Delta intra}$ and MCF7-NRGβ3-like cell lines. However, the latter two cell lines retained normal responsiveness to exogenous NRG, as indicated by the efficient level of tyrosine phosphorylation of the ErbB receptors and the phosphorylation of Akt and Erk1/2 in response to exogenously added soluble NRG.

The failure of MCF7-NRG$^{\Delta intra}$ cells to proliferate raised the question of whether this lack of activity could be due to instability of this mutant as compared with wild type pro-NRGα2c. To explore such a possibility, pulse-chase as well as doxycycline repression experiments were performed. For the pulse-chase experiments, MCF7 cells expressing pro-NRGα2c or pro-NRG$^{\Delta intra}$ were metabolically labeled with ^{35}S-amino acids for 20 min and then chased in normal culture medium for different

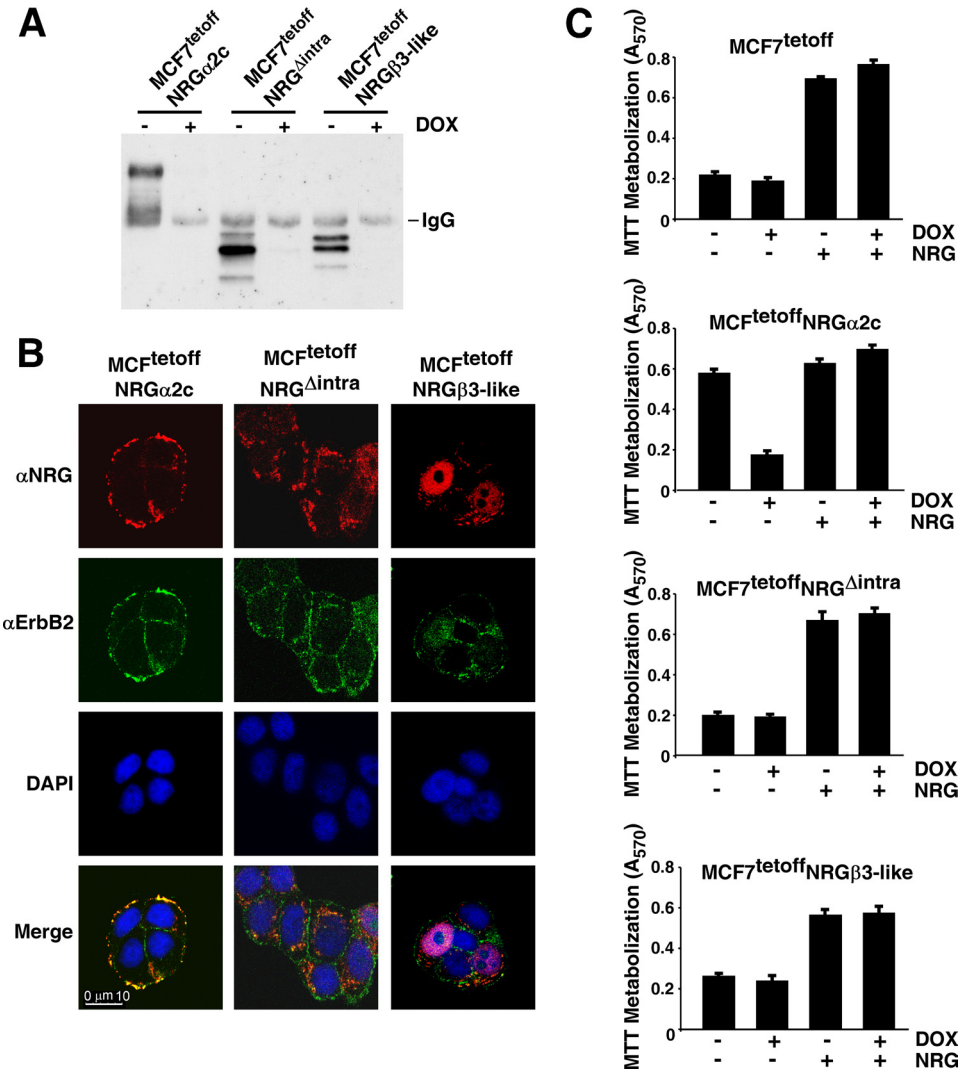

FIGURE 4. **Biological activity of the different pro-NRGα2c mutants.** *A*, expression of the different mutants of pro-NRGα2c in MCF7^{tetoff} cells. Clones of MCF7^{tetoff} expressing the different mutants of pro-NRGα2c (MCF7^{tetoff}-NRGα2c, MCF7^{tetoff}-NRG$^{\Delta intra}$, and MCF7^{tetoff}-NRGβ3-like) were cultured with or without doxycycline (*DOX*; 10 ng/ml) for 2 days and lysed. The samples were analyzed by Western blot with the anti-ectodomain antibody. *B*, subcellular distribution of pro-NRGα2c mutants in MCF7^{tetoff} cells was analyzed by immunofluorescence using the anti-ectodomain antibody. ErbB2 receptor distribution was assessed by immunofluorescence with the 4D5 antibody. *C*, proliferation of MCF7^{tetoff}, MCF7^{tetoff}-NRGα2c, MCF7^{tetoff}-NRG$^{\Delta intra}$, and MCF7^{tetoff}-NRGβ3-like cells. Cells cultured in the presence or absence of doxycycline (10 ng/ml) were treated with or without NRG (10 nM), and MTT metabolization was measured 3 days later. Results are presented as the mean ± S.D. of quadruplicates of an experiment that was repeated twice.

times. As shown in Fig. 5*C* and in agreement with previously published data (17), wild type pro-NRGα2c was initially synthesized as two forms of 70 and 72 kDa, which were rapidly converted into mature forms of higher M_r (~80 kDa), whose amount progressively decreased. Pro-NRG$^{\Delta intra}$ was synthesized as a band of 44 kDa (Fig. 5*C*) whose amount also decreased over time. Quantitative analyses indicated analogous half-lives for pro-NRGα2c and pro-NRG$^{\Delta intra}$ (Fig. 5*D*). We also explored the half-lives of the two proteins upon repression of their mRNAs by doxycycline in the MCF7^{tetoff} cellular model. The addition of doxycycline caused a progressive loss of both pro-NRGα2c and pro-NRG$^{\Delta intra}$ (Fig. 5*E*). The decrease in their amount upon doxycycline-mediated repression followed a similar time course, as indicated by quantitative analyses of the blots (Fig. 5*F*). Together, the above data demonstrate that the half-lives of both proteins were similar, indicating that the differences in their biological properties could not be caused by distinct stability properties of pro-NRG$^{\Delta intra}$ as compared with wild type pro-NRGα2c.

Pro-NRGα2c May Act in Cis at the Plasma Membrane—The above results demonstrated that cell surface exposure of pro-NRGα2c was required for its action and indicated that intracellularly trapped pro-NRG was unable to activate its receptors. A scenario that could explain this behavior could be that of pro-NRG being only able to activate ErbB receptors on neighboring cells (in *trans*) but not the self ErbB receptors (in *cis*). That transmembrane pro-NRG is able to activate receptors in *trans* has already been reported (17, 24). We therefore explored here whether pro-NRG could also act in *cis*. For these experiments, we employed several strategies. First, we used an intracellularly GFP-tagged form of pro-NRG and analyzed whether such a form was able to interact with ErbB3, which acts as its major receptor in MCF7 cells, or activated ErbB2, which forms oligomeric complexes with ErbB3 upon binding of pro-NRG to

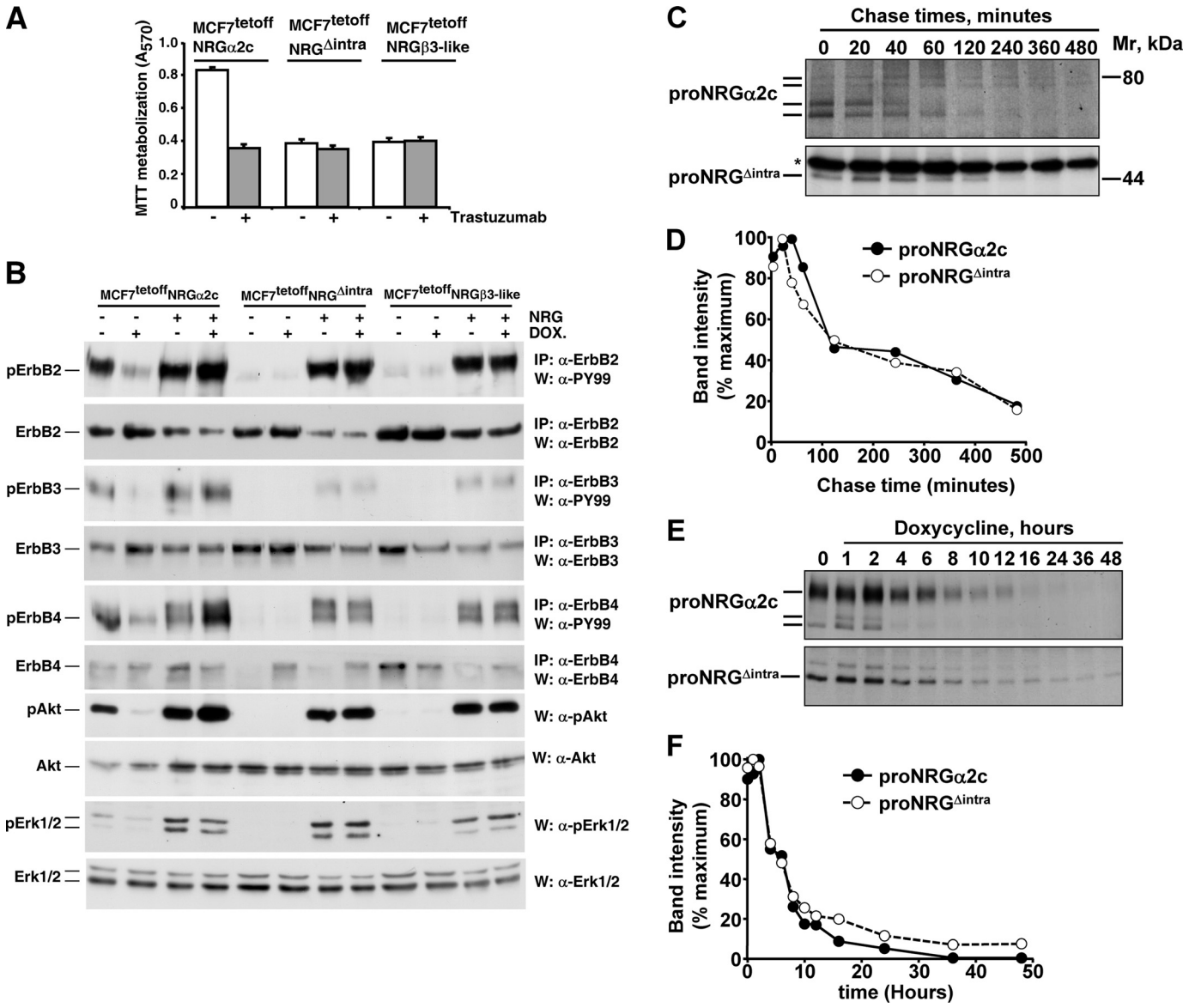

FIGURE 5. **Cell surface pro-NRGα2c activates signaling through ErbB receptors and is sensitive to trastuzumab.** *A*, MCF7^{tetoff}-NRGα2c, MCF7^{tetoff}-NRG$^{\Delta intra}$, and MCF7^{tetoff}-NRGβ3-like cells were plated and treated with or without trastuzumab (50 nM). MTT metabolization was measured 3 days later. Results are presented as the mean ± S.D. (*error bars*) of quadruplicates of an experiment that was repeated twice. *B*, MCF7^{tetoff}-NRGα2c, MCF7^{tetoff}-NRG$^{\Delta intra}$, and MCF7^{tetoff}-NRGβ3-like cells cultured in the presence or absence of doxycycline (10 ng/ml) and treated with or without NRG (10 nM) for 15 min were lysed. Immunoprecipitation (*IP*) (where pertinent) and Western blot (*W*) were performed with the indicated antibodies. *C*, pulse-chase analyses of pro-NRGα2c and pro-NRG$^{\Delta intra}$. Cells were labeled with 200 μCi/ml of a mixture of [^{35}S]cysteine and [^{35}S]methionine for 20 min, and then the medium was replaced by fresh complete medium. Cells were lysed at the indicated times. The extracts were immunoprecipitated with the anti-endodomain (for pro-NRGα2c) or anti-NRG (for pro-NRG$^{\Delta intra}$) antibodies and analyzed in 8 or 10% SDS-polyacrylamide gels, followed by autoradiography. *D*, the graphic shows the percentage of intensity of the sum of the bands of pro-NRGα2c or pro-NRG$^{\Delta intra}$ with respect to the maximum value. *E*, MCF7^{tetoff}-NRGα2c or MCF7^{tetoff}-NRG$^{\Delta intra}$ cells, cultured in the presence of doxycycline (10 ng/ml) for the times indicated, and lysates were analyzed for expression of pro-NRGα2c and pro-NRG$^{\Delta intra}$ by Western blotting with the anti-endodomain or anti-NRG antibodies, respectively. *F*, the graphic shows the percentage of intensity of the sum of the bands of pro-NRGα2c or pro-NRG$^{\Delta intra}$ with respect to the maximum value.

ErbB3 (schematically represented in Fig. 6*A*). Fluorescence microscopy verified a correct membrane exposure of pro-NRG-GFP, indicating that the addition of the extra GFP sequence apparently did not affect expression of that protein to the plasma membrane (Fig. 6*B*). Individualized MCF7 cells expressing NRG-GFP were analyzed for FRET using NRG-GFP as a donor and Alexa 546-labeled anti-ErbB3 or anti-pErbB2 as acceptors. FRET measurements indicated transfer of energy between NRG-GFP and an Alexa 546-labeled antibody that recognized ErbB3 (Fig. 6*C*). In addition, energy transfer between NRG-GFP and an Alexa 546-labeled anti-pErbB2 antibody could also be detected (Fig. 6*D*). Incorporation of the metalloprotease inhibitor TAPI-2 to prevent cleavage of membrane-bound pro-NRG did not substantially affect these data, indicating that no major processing of NRG-GFP was taking place along these experiments. Importantly, no energy transfer was observed when the same experiments were carried out analyzing NRG-GFP at the Golgi cisternae, indicating that although pro-NRG and the receptors are expected to travel through the same intracellular compartments while en route to the mem-

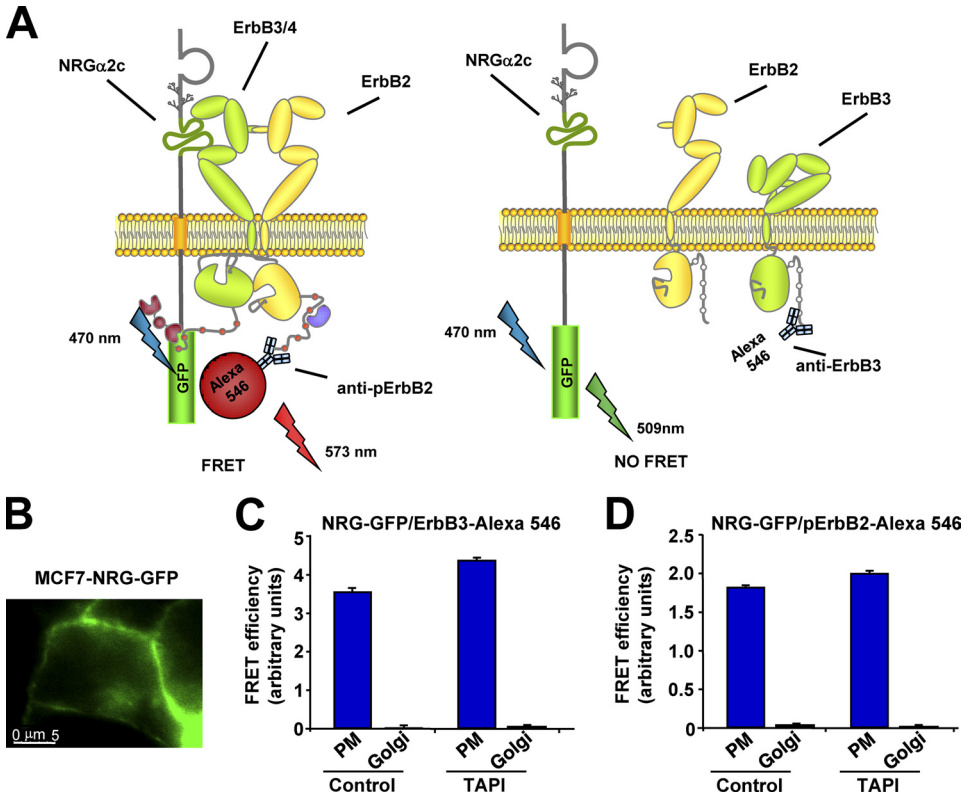

FIGURE 6. **pro-NRGα2c may act in *cis* at the plasma membrane.** *A*, schematic representation of FRET experiments. NRG-GFP was excited with the argon 470-nm laser line. If the intracellular domain of ErbB receptors is close enough, energy is transferred to Alexa 546 anti-pErbB2 or anti-ErbB3 antibodies can be detected at 573 nm. *B*, expression of NRG-GFP at the plasma membrane. Shown is FRET energy transfer between NRG-GFP and Alexa 546-conjugated ErbB3 (*C*) or Alexa 546-conjugated pErbB2 (*D*). Where indicated, TAPI-2 (*TAPI*; 10 μM) was added to the culture medium. FRET measurements were made at the plasma membrane or at the Golgi complex. The results shown are the mean ± S.D. (*error bars*) of three independent experiments.

brane, the productive ligand-receptor interaction occurs only at the plasma membrane.

Further evidence to support this latter conclusion was searched by biochemical analyses of ErbB receptor activation in cells forced to retain ErbB receptors and pro-NRGα2c in intracellular compartments in MCF7 cells. For these experiments, we used brefeldin A, which prevents sorting of proteins from the ER and Golgi to the plasma membrane (35). Treatment with this compound caused a clear redistribution of both pro-NRGα2c and ErbB2 from the plasma membrane to intracellular vesicles that surrounded the nuclear compartment (Fig. 7*A*). As reported previously (17, 18), treatment with brefeldin A affected the electrophoretic mobility of the wild type pro-NRGα2c because, by interfering with the passage of pro-NRGα2c through intracellular membranes, it affects the maturation of the pro-NRGα2c oligosaccharide chains (Fig. 7*B*). This treatment also affected the pattern of the pro-NRG$^{\Delta intra}$. Brefeldin A treatment strongly decreased pErbB2 and pErbB3 levels in MCF7-NRGα2c cells when compared with untreated cells (Fig. 7*C*). Moreover, intracellular retention of ErbB2 did not favor its activation in MCF7-NRG$^{\Delta intra}$ cells. This conclusion was further investigated by FRET analyses of the interaction between NRG and ErbB3 or ErbB2 in cells treated with brefeldin A, which was used to force entrapment of NRG, ErbB3, and ErbB2 in intracellular compartments. Given the precedent that treatment with brefeldin A resulted in loss of pErbB2 (Fig. 7*C*), the potential existence of pro-NRGα2c-ErbB2 interactions was analyzed using anti-ErbB2 instead of anti-pErbB2 antibodies. These experiments confirmed the lack of interaction between pro-NRG and ErbB3 or ErbB2 (Fig. 7, *D* and *E*, respectively) in the intracellular compartments even when colocalization between the pro-NRG and the ErbB receptors was forced by brefeldin A. Together, these data indicate that intracellular pro-NRGα2c is unable to interact with the ErbB receptors, at least in a productive manner. However, the FRET experiments indicated that pro-NRG could act on self receptors (in *cis*) but only when both the transmembrane factors and the receptors are exposed at the cell surface.

DISCUSSION

A unique structural property of most type I transmembrane pro-NRGs is their absence of an N-terminal signal sequence. This characteristic raises the question of what regions of these pro-NRGs are required for their membrane anchoring and targeting to the plasma membrane. Previous reports suggested that the internal hydrophobic region could act as a signal sequence due to the failure to detect NRGβ3, which lacks this region, in the extracellular medium (15). The studies presented here with the different pro-NRGα2c mutants indicate that in fact, the internal hydrophobic region of pro-NRGα2c may act as an internal signal sequence. Moreover, we report that this region is responsible for the membrane-anchoring properties of type I transmembrane NRGs. In fact, elimination of the extracellular or intracellular domains of pro-NRGα2c preserving this internal hydrophobic region resulted in mutant forms that associated with microsomal membranes. Interestingly,

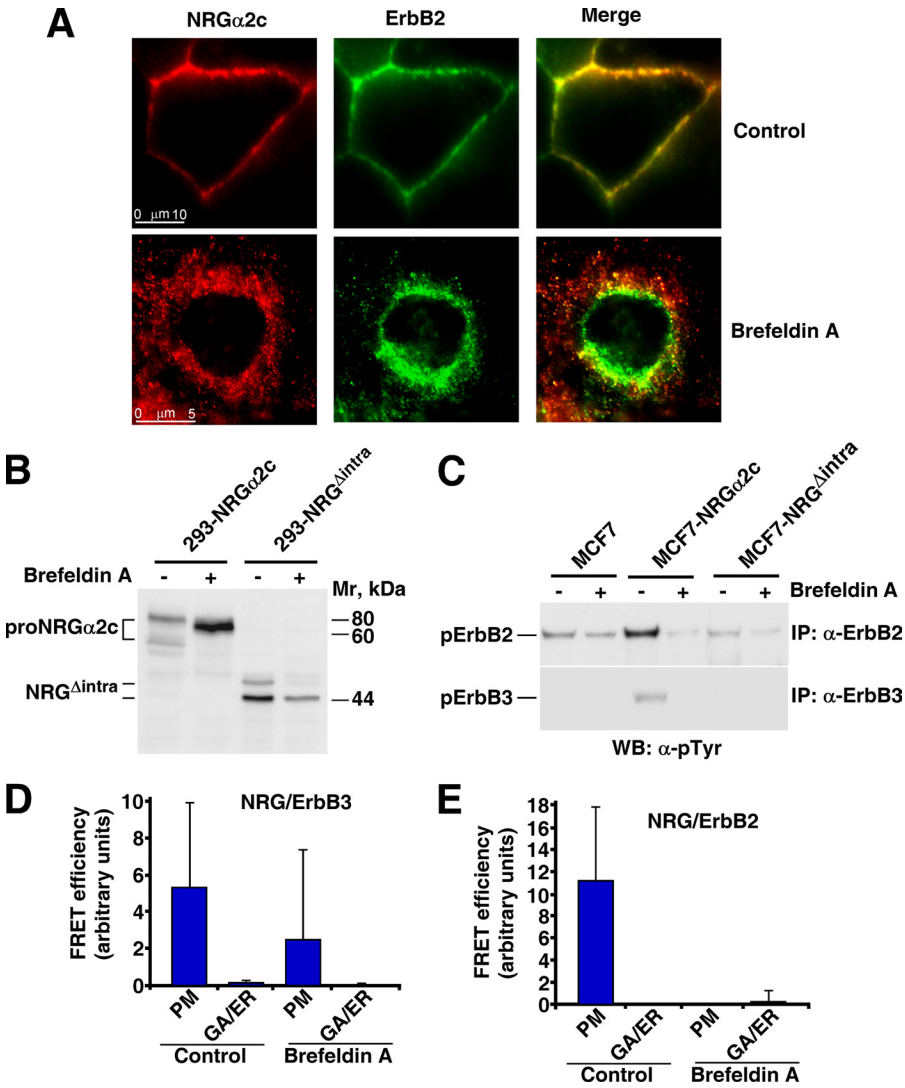

FIGURE 7. **Intracellular pro-NRGα2c fails to activate ErbB receptors.** *A*, subcellular distribution of pro-NRGα2c and ErbB2 in MCF7 cells treated with brefeldin A. MCF7 cells were cultured on coverslips and 1 day later were treated with or without brefeldin A (10 μg/ml) overnight. *B*, effect of brefeldin A on pro-NRGα2c and the pro-NRG$^{\Delta intra}$ mutant. The extracts were immunoprecipitated and analyzed by Western blot with the anti-ectodomain antibodies. *C*, MCF7, MCF7-NRGα2c, and MCF7-NRG$^{\Delta intra}$ cells treated with brefeldin A overnight were lysed. The extracts were immunoprecipitated (*IP*) with the anti-ErbB2 or anti-ErbB3 antibodies, and Western blot (*WB*) was performed with the anti-phosphotyrosine (*α-pTyr*) antibody. Shown are FRET analyses of the interactions between NRG and ErbB3 (*D*) and between NRG and ErbB2 (*E*). Where indicated, brefeldin A (10 μg/ml) was added to the culture medium overnight. FRET measurements were made at the plasma membrane or in intracellular compartments (*GA/ER*). The results shown are the mean ± S.D. (*error bars*) of three independent experiments.

some of these mutants failed to reach the plasma membrane, as indicated by the protease protection experiments, the cytometry, or the immunofluorescent stainings. Thus, deletion of the intracellular domain of pro-NRGα2c created a mutant form of the protein that retained membrane anchoring capability but was unable to reach the plasma membrane. This finding suggests that the internal hydrophobic region of pro-NRGα2c confers membrane-anchoring properties but is not sufficient to provide cell surface targeting properties. It also indicates that the intracellular domain of pro-NRGα2c is required for its adequate sorting to the plasma membrane. Importantly, the C terminus of pro-NRGα2c includes a valine residue that could play a role in directing pro-NRGα2c to the plasma membrane, in analogy to the critical role that C-terminal intracellular valines play in the adequate sorting of the related EGF family member pro-TGFα (36, 37).

Deletion of the extracellular domain of pro-NRGα2c resulted in a mutant protein that associated with the microsomal fraction and apparently was correctly targeted to the cell surface. This indicates that the extracellular region of pro-NRGα2c is not required for the sorting to the plasma membrane and suggests that the transmembrane and intracellular regions of pro-NRGα2c may be sufficient to confer membrane-anchoring and cell surface-targeting properties to pro-NRGs but not to any protein. In fact, the chimeric ERK5-NRG proteins showed targeting of these chimeric proteins to microsomes, further confirming that the internal hydrophobic region conferred membrane-anchoring properties. However, these chimeras failed to reach the cell surface, indicating that the transmembrane and intracellular regions do not have sufficient strength to move any sequence to the plasma membrane and therefore require a permissive extracellular sequence to move the protein to that location.

Accumulation of pro-NRG$^{\Delta intra}$ in intracellular microsomal compartments offered the possibility to explore whether at such a location this pro-NRG form was active. This was an important aspect of our research because former studies carried out with mutant forms of pro-EGF indicated that intracellular entrapment of EGF was able to activate the EGF receptor in an intracrine manner (25–27). Expression of pro-NRG$^{\Delta intra}$ in MCF7 cells was unable to activate NRG receptors, indicating that intracellular NRG is unable to activate the ErbB receptors. The failure to activate ErbB receptors at this intracellular location is unknown. Because pro-NRGs and the ErbB receptors are transmembrane proteins that move to the cell surface, they are expected to share the export machinery, and it is therefore likely that they coincide with each other along the secretory pathway responsible for their targeting to the plasma membrane. In MCF7 cells, ErbB2 and ErbB3, although traveling through the same compartments as pro-NRG, are not easily detected in these intracellular sites by regular immunofluorescence techniques, indicating that their export to the surface is efficient, probably more than that of pro-NRG, which may be detected at the Golgi cisternae. The rapid movement to the membrane may therefore restrict the time that the ErbB receptors reside in intracellular sorting compartments, diminishing access to pro-NRG, and this could explain the lack of activation of ErbB receptors in cells expressing pro-NRG$^{\Delta intra}$. We attempted to force such an intracellular interaction with brefeldin A. Treatment with this compound failed to increase ErbB2 and ErbB3 phosphorylation in cells expressing pro-NRG$^{\Delta intra}$. Moreover, this drug caused inhibition of ErbB2 and ErbB3 tyrosine phosphorylation in cells expressing wild type pro-NRGα2c. In addition, FRET experiments failed to detect interaction between pro-NRGα2c and its receptors in intracellular compartments, even under conditions, such as brefeldin A treatment, that force retention of the ligand and the receptors probably in the same intracellular compartments. These results indicate that in intracellular compartments, transmembrane NRG is signaling-incompetent. Such a failure to activate ErbB receptors may be caused by segregation of the receptor and the ligands in these intracellular compartments or by deficient pro-NRG-ErbB interaction due to intrinsic characteristics of these compartments, such as low lumenal pH. Another possibility that may explain the failure of intracellular pro-NRG to activate ErbB receptors is incomplete maturation of the membrane-bound factor at these intracellular sites. It is also possible that the failure of the pro-NRG$^{\Delta intra}$ to stimulate MCF7 proliferation could be due to instability of this protein with respect to wild type pro-NRGα2c. The half-lives of both proteins were found to be similar, as indicated by the pulse-chase radioactive experiments as well as results obtained in the doxycycline-regulatable cell models. It is therefore unlikely that different stabilities of both proteins may explain their distinct biological properties.

From the physiological point of view, our results help in explaining the failure of pro-NRG mutants with deletion in the intracellular domain to carry out their function during development (38, 39). Liu *et al.* (38, 39) reported a role of the NRG tail in animal development because mice expressing a pro-NRG$^{\Delta intra}$-like form presented a phenotype analogous to NRG null mice. The authors suggested that this form was unable to dimerize, and this could result in its deficient cleavage and solubilization. Our results suggest that deficient release of soluble NRG in pro-NRG$^{\Delta intra}$-expressing cells is due to lack of cell surface exposure; the site where the protease that cleaves the ectodomain of pro-NRGs is active (17, 18).

Another question that we addressed was whether transmembrane ligands can activate their receptors in *cis*. Previous studies have already demonstrated that pro-NRGs may activate ErbB receptors in a juxtacrine manner (in *trans*) (9, 17, 24). In isolated MCF7 cells expressing pro-NRGα2c, FRET measurements showed interaction of ErbB3 and pErbB2 with pro-NRGα2c but only when the factor and the receptor were present at the plasma membrane. This indicates that pro-NRGα2c may activate ErbB receptors located in the same cell that produces the ligand, in addition to acting on receptors located in cells that are in physical contact with the growth factor-producing cell. We term this transautocrine stimulation, to indicate this binary potential of action of a transmembrane growth factor on receptors. Although the soluble crystals of NRG with the ectodomain of their receptors have been solved (40), these structures cannot answer at present how a transmembrane factor may interact with ErbB receptors in a transautocrine manner. It appears likely that both the membrane factor and the receptor must have a substantial degree of flexibility to be able to interact at the plasma membrane, especially considering that the ligand binding regions are shared between subdomains I and III of the receptors. We are expecting structural studies that will define how a membrane-anchored pro-NRG may interact with its receptors.

In conclusion, our work has established that the internal hydrophobic region of type I transmembrane NRGs is competent to act as a membrane-anchoring and signal sequence domain. Our findings also allowed dissection between membrane-anchoring and cell surface-targeting properties of these pro-NRGs. In addition, we offer for the first time evidence indicating that transmembrane growth factors may activate their receptors in *cis*. These findings contribute to a better understanding of the biological properties of membrane-anchored growth factors that may be useful in the design of therapeutic strategies for diseases involving transmembrane NRGs.

REFERENCES

1. Falls, D. L. (2003) *Exp. Cell Res.* **284,** 14–30
2. Lemke, G. (1996) *Mol. Cell. Neurosci.* **7,** 247–262
3. Meyer, D., and Birchmeier, C. (1995) *Nature* **378,** 386–390
4. Britsch, S., Li, L., Kirchhoff, S., Theuring, F., Brinkmann, V., Birchmeier, C., and Riethmacher, D. (1998) *Genes Dev.* **12,** 1825–1836
5. Mei, L., and Xiong, W. C. (2008) *Nat. Rev. Neurosci.* **9,** 437–452
6. Wolpowitz, D., Mason, T. B., Dietrich, P., Mendelsohn, M., Talmage, D. A., and Role, L. W. (2000) *Neuron* **25,** 79–91
7. Montero, J. C., Rodríguez-Barrueco, R., Ocaña, A., Díaz-Rodríguez, E., Esparís-Ogando, A., and Pandiella, A. (2008) *Clin. Cancer Res.* **14,** 3237–3241
8. Breuleux, M. (2007) *Cell. Mol. Life Sci.* **64,** 2358–2377
9. Yuste, L., Montero, J. C., Esparís-Ogando, A., and Pandiella, A. (2005) *Cancer Res.* **65,** 6801–6810
10. Atlas, E., Cardillo, M., Mehmi, I., Zahedkargaran, H., Tang, C., and Lupu, R. (2003) *Mol. Cancer Res.* **1,** 165–175
11. Tsai, M. S., Shamon-Taylor, L. A., Mehmi, I., Tang, C. K., and Lupu, R. (2003) *Oncogene* **22,** 761–768

12. Krane, I. M., and Leder, P. (1996) *Oncogene* **12,** 1781–1788
13. de Alava, E., Ocaña, A., Abad, M., Montero, J. C., Esparís-Ogando, A., Rodríguez, C. A., Otero, A. P., Hernández, T., Cruz, J. J., and Pandiella, A. (2007) *J. Clin. Oncol.* **25,** 2656–2663
14. Massagué, J., and Pandiella, A. (1993) *Annu. Rev. Biochem.* **62,** 515–541
15. Wen, D., Suggs, S. V., Karunagaran, D., Liu, N., Cupples, R. L., Luo, Y., Janssen, A. M., Ben-Baruch, N., Trollinger, D. B., and Jacobsen, V. L. (1994) *Mol. Cell. Biol.* **14,** 1909–1919
16. Burgess, T. L., Ross, S. L., Qian, Y. X., Brankow, D., and Hu, S. (1995) *J. Biol. Chem.* **270,** 19188–19196
17. Montero, J. C., Rodríguez-Barrueco, R., Yuste, L., Juanes, P. P., Borges, J., Esparís-Ogando, A., and Pandiella, A. (2007) *Mol. Biol. Cell* **18,** 380–393
18. Montero, J. C., Yuste, L., Díaz-Rodríguez, E., Esparís-Ogando, A., and Pandiella, A. (2000) *Mol. Cell. Neurosci.* **16,** 631–648
19. Carraway, K. L., 3rd, Weber, J. L., Unger, M. J., Ledesma, J., Yu, N., Gassmann, M., and Lai, C. (1997) *Nature* **387,** 512–516
20. Harari, D., Tzahar, E., Romano, J., Shelly, M., Pierce, J. H., Andrews, G. C., and Yarden, Y. (1999) *Oncogene* **18,** 2681–2689
21. Hayes, N. V., Newsam, R. J., Baines, A. J., and Gullick, W. J. (2008) *Oncogene* **27,** 715–720
22. Zhang, D., Sliwkowski, M. X., Mark, M., Frantz, G., Akita, R., Sun, Y., Hillan, K., Crowley, C., Brush, J., and Godowski, P. J. (1997) *Proc. Natl. Acad. Sci. U.S.A.* **94,** 9562–9567
23. Thorne, B. A., and Plowman, G. D. (1994) *Mol. Cell. Biol.* **14,** 1635–1646
24. Aguilar, Z., and Slamon, D. J. (2001) *J. Biol. Chem.* **276,** 44099–44107
25. Wiley, H. S., Woolf, M. F., Opresko, L. K., Burke, P. M., Will, B., Morgan, J. R., and Lauffenburger, D. A. (1998) *J. Cell Biol.* **143,** 1317–1328
26. Dong, J., Opresko, L. K., Chrisler, W., Orr, G., Quesenberry, R. D., Lauffenburger, D. A., and Wiley, H. S. (2005) *Mol. Biol. Cell* **16,** 2984–2998
27. Maheshwari, G., Wiley, H. S., and Lauffenburger, D. A. (2001) *J. Cell Biol.* **155,** 1123–1128
28. Esparís-Ogando, A., Díaz-Rodríguez, E., Montero, J. C., Yuste, L., Crespo, P., and Pandiella, A. (2002) *Mol. Cell. Biol.* **22,** 270–285
29. Sambrook, J., Fritsch, E. F., and Maniatis, T. (1989) *Molecular Cloning: A Laboratory Manual*, 2nd Ed., pp. 16.32–16.36, Cold Spring Harbor Laboratory, Cold Spring Harbor, NY
30. Cabrera, N., Díaz-Rodríguez, E., Becker, E., Martín-Zanca, D., and Pandiella, A. (1996) *J. Cell Biol.* **132,** 427–436
31. Massagué, J. (1983) *J. Biol. Chem.* **258,** 13614–13620
32. Borges, J., Pandiella, A., and Esparís-Ogando, A. (2007) *Cell. Signal.* **19,** 1473–1487
33. Agus, D. B., Akita, R. W., Fox, W. D., Lewis, G. D., Higgins, B., Pisacane, P. I., Lofgren, J. A., Tindell, C., Evans, D. P., Maiese, K., Scher, H. I., and Sliwkowski, M. X. (2002) *Cancer Cell* **2,** 127–137
34. Holmes, W. E., Sliwkowski, M. X., Akita, R. W., Henzel, W. J., Lee, J., Park, J. W., Yansura, D., Abadi, N., Raab, H., Lewis, G. D., Shepard, H. M., Kuang, W. J., Wood, W. I., Goeddel, D. V., and Vandlen, R. L. (1992) *Science* **256,** 1205–1210
35. Klausner, R. D., Donaldson, J. G., and Lippincott-Schwartz, J. (1992) *J. Cell Biol.* **116,** 1071–1080
36. Bosenberg, M. W., Pandiella, A., and Massagué, J. (1992) *Cell* **71,** 1157–1165
37. Fernández-Larrea, J., Merlos-Suárez, A., Ureña, J. M., Baselga, J., and Arribas, J. (1999) *Mol. Cell* **3,** 423–433
38. Liu, X., Hwang, H., Cao, L., Buckland, M., Cunningham, A., Chen, J., Chien, K. R., Graham, R. M., and Zhou, M. (1998) *Proc. Natl. Acad. Sci. U.S.A.* **95,** 13024–13029
39. Liu, X., Hwang, H., Cao, L., Wen, D., Liu, N., Graham, R. M., and Zhou, M. (1998) *J. Biol. Chem.* **273,** 34335–34340
40. Burgess, A. W., Cho, H. S., Eigenbrot, C., Ferguson, K. M., Garrett, T. P., Leahy, D. J., Lemmon, M. A., Sliwkowski, M. X., Ward, C. W., and Yokoyama, S. (2003) *Mol. Cell* **12,** 541–552